Sound propagation in dense, frictional granular materials

O. Mouraille & S. Luding
Particle Technology, DelftChemTech, Julianalaan 136, 2628 BL Delft, Netherlands

ABSTRACT: The understanding of the sound propagation mechanisms (dispersion, scattering, power-spectra, etc.) inside dense granular matter is still a challenge. Using discrete element simulations we examine the effect of interparticle forces like friction and thus also the role of rotations. A small perturbation is created on one side of a dense, static packing of grains and then examined during propagation and when arriving at the opposite side. The perturbations can be applied to longitudinal, shear or rotational degrees of freedom in order to select the respective modes of information propagation. In order to bridge the gap between the particle "micro"-method and the "macroscopic" continuum theory, we use a micro-macro approach for finding relations between the wave speeds and the components of the stiffness tensor.

1 INTRODUCTION

The mechanisms of wave propagation through a given material are strongly related to the properties of this material, like the stiffness and the structure (where anisotropy comes into play), but also are related to phenomena like dissipation, including friction, as well as temperature changes (Liu & Nagel 1992). When using discrete element simulations one can define local contact parameters for the material and tune them in order to examine their particular effect. Nevertheless, for applications on large scale, the material obtained with the simulation has to be described with a continuum theory and its related variables (e.g. bulk- and shear-modulus). This points out a more general problem: The "micro-macro" transition for granular materials. In this paper the influence of friction and the difference between modes of propagation (compressive/shear) are examined by comparing the pressure evolution at both sender and receiver walls. Also the ratio of the two wave speeds (compressive and shear) of an anisotropic packing is compared with the ratio of the two corresponding components of the stiffness tensor (obtained by our micro-macro approach) (Vermeer et al. 2001; Kishino 2001).

2 DESCRIPTION OF THE MODEL

The discrete element model (DEM) (Cundall & Strack 1979; Herrmann et al. 1998; Oda & Iwashita 2000; Thornton & Antony 2000) is briefly introduced in this section, together with a brief description of the model system; for more details see (Luding 2004).

2.1 *Discrete Particle Model*

The elementary units of granular materials are mesoscopic grains which deform under the stress developing at their contacts. Since the realistic modeling of the internal deformations of the particles is much too complicated, we relate the normal interaction force to the overlap δ of two spherical particles. If all forces $\boldsymbol{f}_i$, acting on particle i, either from other particles, from boundaries or from external forces, are known, the problem is reduced to the integration of Newton's equations of motion for the translational and rotational degrees of freedom

$$m_i \frac{\mathrm{d}^2}{\mathrm{d}t^2}\boldsymbol{r}_i = \boldsymbol{f}_i \ , \quad \text{and} \quad I_i \frac{\mathrm{d}^2}{\mathrm{d}t^2}\boldsymbol{\varphi}_i = \boldsymbol{t}_i \ , \qquad (1)$$

with the mass m_i of particle i, its position $\boldsymbol{r}_i$ the total force $\boldsymbol{f}_i = \sum_c \boldsymbol{f}_i^c$ acting on it due to contacts with other particles or with the walls, its moment of inertia I_i, its angular velocity $\boldsymbol{\omega}_i = \mathrm{d}\boldsymbol{\varphi}_i/\mathrm{d}t$ and the total torque $\boldsymbol{t}_i$.

Linear normal contact law:
The force acting on particle i from particle j can be decomposed into a normal and a tangential part, where the simplest normal force is a linear spring and a linear dashpot $f_i^n = k\delta + \gamma_0\dot{\delta}$, with spring constant k and some damping coefficient γ_0. The consequences of more realistic normal force laws, involving non-linearities, plastic deformation, and attractive cohesion forces will be discussed elsewhere. The half-period of a (damped) vibration around the equilibrium position can be computed, and one obtains a typical

response time $t_c = \pi/\omega$, with $\omega = \sqrt{(k/m_{ij}) - \eta_0^2}$, the eigenfrequency of the contact, the reduced mass $m_{ij} = m_i m_j/(m_i + m_j)$, and the rescaled damping coefficient $\eta_0 = \gamma_0/(2m_{ij})$. The energy dissipation during a collision, as caused by the dashpot, leads to a (constant) restitution coefficient $r = -v_n'/v_n = \exp(-\eta_0 t_c)$, where the prime denotes the normal velocity after a collision.

Tangential Contact Model:
The force in tangential direction is implemented in the spirit of (Cundall & Strack 1979), where a tangential spring was introduced, in order to account for static friction. Various authors have used this idea and numerous variants were implemented, see (Brendel & Dippel 1998) for a summary and discussion, and (Luding 2004) for a detailed description of the tangential friction force model used (see also the paper by C. David et al. in this book).

2.2 *Model system*

We consider a dense, static packing of grains contained in a cuboidal volume, for which two different configurations have been studied: a regular monodisperse packing and a random polydisperse packing; however, we focus on the regular packing in the following. The packing is bounded by (stress- or strain-controlled) walls (*w*) in a first case, and treated as piece of an infinite, larger sample via periodic boundaries (*pb*) in a second case. Periodic boundaries means here that if a particle exits at one side of the simulation volume it enters at the opposite side at according position with the same velocity.

By applying a small perturbation to the system at one side wall or by moving a layer of particles (depending on the boundary conditions *w* or *pb*, respectively), a wave is created perpendicular to either agitating wall or layer. Both compressive (P) and shear (S) modes of propagation are examined by directing the perturbations either parallel or perpendicular to the wave propagation direction.

The regular monodisperse packing is, in our case, a stack of horizontal square layers, such that, starting from the bottom, each higher layer lies in the holes of the one below, see Fig. 1. This makes the packing similar in the horizontal directions, but different in the third, vertical direction, hence creating an anisotropic system. Random polydisperse packings are typically obtained by compressing the walls of a loose packing, where the particles have a random radius from a given size distribution. Before the sound wave is agitated, the system is relaxed until it reaches a reasonable static equilibrium state, with stress P_0 such that particles overlaps are much smaller than their diameter; in the case of the regular homogeneous packing used in the following, the system can be prepared immediately in a static configuration, whereas a system with polydisperse particles has to be relaxed, which can take much longer than a typical wave propagation simulation.

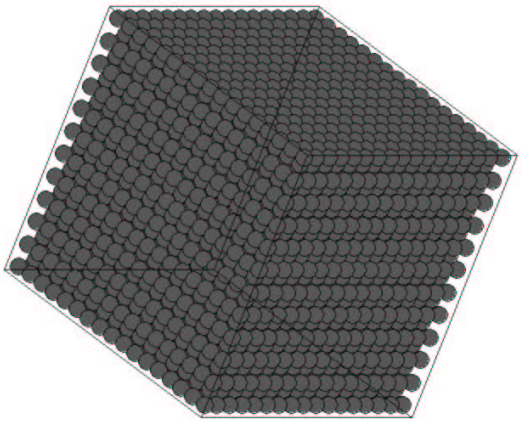

Figure 1. Regular monodisperse packing

The packing used here contains $N \approx 6000$ particles with radius $a = 0.001$m. The mass of the spherical particles is $m = \rho(4/3)\pi a^3$, with the density $\rho = 2.10^3 \mathrm{kg\,m^{-3}}$. The total mass of the system is thus $M \approx 0.0645\,\mathrm{kg}$. The material parameters are $k = 10^5\,\mathrm{N\,m^{-1}}$, $k_t = 0.2k$ (tangential spring stiffness), and $\gamma_0 = 0.04\,\mathrm{kg\,s^{-1}}$. This leads to a typical contact duration $t_c = 2.25\ 10^{-5}\,\mathrm{s}$ and a restitution coefficient of $r = 0.9$. As integration time-step we used $\delta t_{\mathrm{MD}} = 4.10^{-7}\,\mathrm{s}$.

3 SIMULATION RESULTS

In the following, the wave propagation is first examined in systems with walls and varying friction coefficients, starting with smooth, frictionless particles. Then the propagation speeds of different modes (compression/shear) are examined in a system with periodic boundaries.

By simply looking at the pressure as function of time at both agitated and response walls we can already get some information on the wave, see Fig. 2. The motion of the agitation wall leads to a rapid stress increase, which travels into the system towards the opposite wall. Modulations of the stress, much smaller than the agitation peak-stress remain throughout the whole simulation. The receiving wall experiences the increase in stress with a time delay and with much slower rate of change. The wave is reflected from the receiver wall and travels back and forth between agitation and receiver wall several times, ever decreasing in amplitude (data not shown here).

The system size divided by the time difference between the two peaks gives an approximated wave speed. The difference in amplitude (smaller at the response wall) and shape (broader at the response wall) is caracteristic for the wave dispersion. Thus,

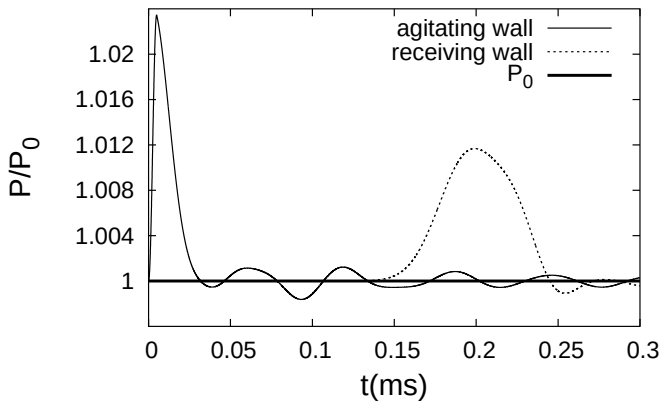

Figure 2. Normal stress (scaled by the equilibrium stress P_0), plotted against time, at both agitated and response walls.

speed, amplitude, and shape already allow for parameter studies and analysis of the wave propagation mechanisms. However, in the following, we focus on the wave-speed for different strength of friction.

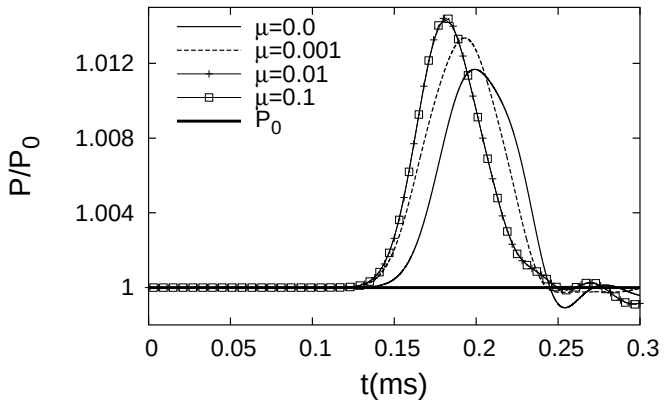

Figure 3. Scaled normal stress plotted against time at the receiver wall, for different friction coefficients μ.

Using the same system as before, we only activate Coulomb friction between the particles, and vary the friction coefficient μ. For the same agitation as before, with some larger amplitude of agitation (larger, but still small enough that no contacts are opened), we focus now on the receiver wall, see Fig. 3. Note that the wave speed seems to be independent of the agitation amplitude – at least for the still small amplitude used. Comparing simulations with different friction strength, first, a difference in the amplitude is visible, and second, stronger friction makes the wave propagate faster. This can be related to the stiffness of the material which is higher with friction, i.e. the stiffness is increased due to the addition of tangential springs in the particle model. The increase in stiffness is rather small due to the small ratio of tangential to normal stiffness $k_t/k_n = 0.2$.

Note that smaller agitation amplitude and larger friction coefficients ($\mu \geq 0.01$) do not lead to different wave-shape or -speed. This is due to the fact that this sample was created without friction, such that at the beginning of the agitation, all contacts have no tangential force, i.e. friction is initially inactive. Perturbation leads to a stretching of tangential springs and – only for small enough friction coefficients – to sliding contacts. If the friction coefficient becomes too large (fixed amplitude), the sliding limit is not reached. Increasing the amplitude (fixed friction coefficient), on the other hand, can lead to sliding contacts. By decreasing the friction coefficient such that certain contacts reach the limit of the Coulomb cone ($\mu = 0.001$), we get something in between the extreme cases.

Assuming that the granular material behaves like an *elastic continuum*, the anisotropic relation between stress- and strain-increments involves a material tensor $\boldsymbol{C}$ of rank four. In symbolic and index notation (Einstein convention with summation over double indices) this reads in incremental form:

$$\dot{\boldsymbol{\sigma}} = \boldsymbol{C} : \dot{\boldsymbol{e}} \ , \quad \text{or} \quad \dot{\sigma}_{ij} = C_{ijkl}\dot{e}_{kl} \ , \tag{2}$$

with the stress- and strain-rates on the left and right respectively. This describes also the response of our packing and implies the assumption of a *constant, time-invariant material tensor*, which can be true only for very *small* deformations, and does not allow for opening or closing of contacts or even large scale rearrangements.

In the isotropic case, continuum theory gives a direct relation (first order approximation) between the wave speeds (P- and S-wave) and the material moduli: $\rho {v_P}^2 = \lambda + 2\mu$ and $\rho {v_S}^2 = \mu$, with v_P and v_S the P- and S-wave speeds, respectively, ρ the bulk material density, and λ, μ the Lamé coefficients in isotropic materials.

In a dense, regular, monodisperse packing, these relations are a reasonable approximation as far as we are in the long-wave limit (wavelength much larger than the particle size). Making the assumption that in our packing (special anisotropy) such relations also hold, we can write: $\rho {v_P}^2 = C_{zzzz}$ and $\rho {v_S}^2 = C_{zxzx}$, for waves propagating in the z-direction. Although the relatively "small" size of our packing does not necessarily allow to reach the long wavelength limit, in order to test our simulation with respect to these relations, we compare the ratios between the wave speeds $(v_P/v_S)^2$, and the related stiffness tensor entries C_{zzzz}/C_{zxzx}.

This comparison is relevant since the dispersion curves for P- and S-wave in a regular lattice have the form: $\omega = v_P \sin(k_d)$, and $\omega = v_P \sin(k_d)$, with ω the angular frequency and k_d the normalized wavenumber. Thus also the ratio of their derivatives, v_P/v_S, does not depend on the wave number, see (Suiker et al. 2001). From the same packing as before, but using now periodic boundaries (for practical reasons), we create a shear wave by shifting a horizontal layer in a horizontal direction (say x). Shifting the

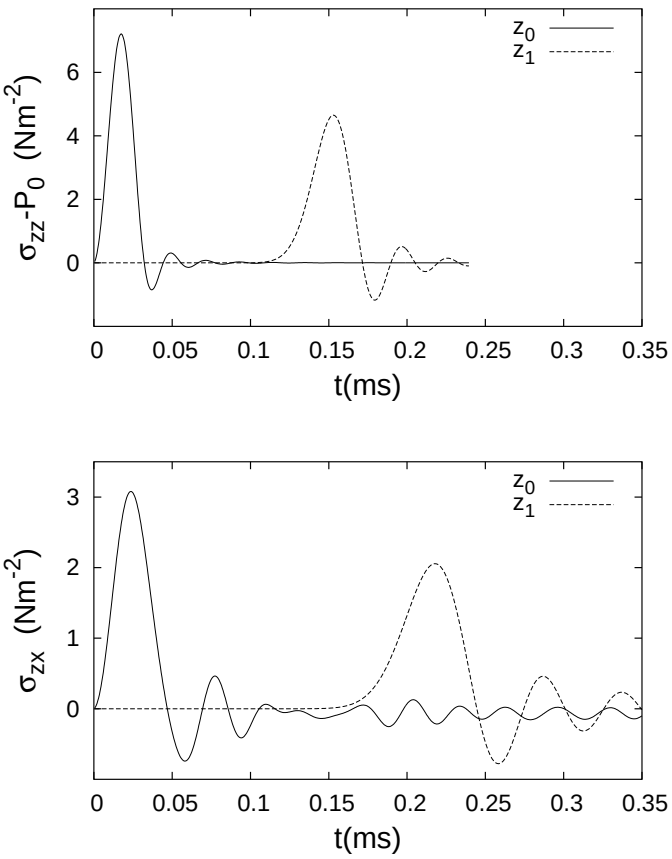

Figure 4. Components of the stress tensor: (Top) σ_{zz} (compressive-wave) and (Bottom) σ_{zx} (shear-wave) as function of time at the shifted layer at z_0 and a second layer at z_1, with $z_1 - z_0 = 0.03\,\mathrm{m}$ (with friction $\mu = 0.5$ and $P_0 \approx 62\,\mathrm{kNm}^{-2}$).

same layer in the direction of propagation (z), we get a compressive wave. The same type of graph as before is obtained (see Fig. 4) by taking the components of the stress tensor averaged in different layers at different times. The stress tensor is calculated according to the standard definition for granular material, for more details concerning the averaging method, see (Luding 2004). From this we get two different speeds $v_P \approx 223\,\mathrm{m\,s}^{-1}$ and $v_S \approx 155\,\mathrm{m\,s}^{-1}$ and the corresponding ratio $v_P^2/v_S^2 \approx 2.07$. On the other hand from a micro-macro approach we can express a macroscopic stiffness tensor for the packing, see (Luding 2004), which gives $C_{zzzz} \approx 66068000\,\mathrm{kg\,m}^{-1}\mathrm{s}^{-2}$ and $C_{zxzx} \approx 33034000\,\mathrm{kg\,m}^{-1}\mathrm{s}^{-2}$, with the ratio $C_{zzzz}/C_{zxzx} \approx 2$ (with volume density $\nu \approx 0.74$). We observe thus a nice agreement between the two ratios.

4 CONCLUSION

In this paper we showed the results of three dimensional simulations for wave propagation in a dense, static, regular, monodisperse packing of spheres, for different propagation modes, compressive (P) and shear (S), and also in the case of the P-wave for different friction coefficients. We compared the ratios of the P- and S-wave speeds, v_P^2/v_S^2 with the corresponding stiffness ratios and obtained quantitative agreement, although we only looked at the normal contributions for the stiffness tensor. This indicate the consistency between our model and classical theory in regular homogeneous packings, and thus is the first step towards the understanding of wave propagation in polydisperse, inhomogeneous, anisotropic, dense, frictional granular materials.

ACKNOWLEDGEMENTS

Helpful discussions with G. Herman, W. Mulders, and A. Suiker are appreciated. This work is part of the research programme of the Stichting voor Fundamenteel Onderzoek der Materie (FOM), financially supported by the Nederlandse Organisatie voor Wetenschappelijk Onderzoek (NWO) and the Stichting Shell Research.

REFERENCES

Brendel, L. & Dippel, S. 1998. Lasting contacts in molecular dynamics simulations. In H. J. Herrmann, J.-P. Hovi, & S. Luding (eds), *Physics of Dry Granular Media*: Dordrecht: 313. Kluwer Academic Publishers.

Cundall, P. A. & Strack, O. D. L. 1979. A discrete numerical model for granular assemblies. *Géotechnique 29*(1): 47–65.

Herrmann, H. J., Hovi, J.-P., & Luding, S. (eds) 1998. *Physics of dry granular media - NATO ASI Series E 350*: Dordrecht. Kluwer Academic Publishers.

Kishino, Y. (ed.) 2001. *Powders & Grains 2001*: Rotterdam. Balkema.

Liu, C. & Nagel, S. R. 1992. Sound in sand. *Phys. Rev. Lett. 68*(15): 2301–2304.

Luding, S. 2004. Micro-macro transition for anisotropic, frictional granular packings. *Int. J. Sol. Struct.* 41: 5821–5836.

Oda, M. & Iwashita, K. 2000. Study on couple stress and shear band development in granular media based on numerical simulation analyses. *Int. J. of Enginering Science* 38: 1713–1740.

Suiker, A. S. J., Metrikine, A. V., & de Borst, R. 2001. Comparison of wave propagation characterisitcs of the cosserat continuum model and corresponding discrete lattice models. *Int. J. of Solids and Structures* 38: 1563–1583.

Thornton, C. & Antony, S. J. 2000. Quasi-static deformation of a soft particle system. *Powder Technology 109*(1-3): 179–191.

Vermeer, P. A., Diebels, S., Ehlers, W., Herrmann, H. J., Luding, S., & Ramm, E. (eds) 2001. *Continuous and Discontinuous Modelling of Cohesive Frictional Materials*: Berlin. Springer. Lecture Notes in Physics 568.